

Oscillations and bistability in the dynamics of cytotoxic reactions mediated by the response of immune cells to solid tumours

O. Lejeune^a, M.A.J. Chaplain^{a,*}, I. El Akili^b

^a *The SIMBIOS Centre, Department of Mathematics, University of Dundee, Dundee DD1 4HN, Scotland, United Kingdom*

^b *Faculté des Sciences, CP 231, Université Libre de Bruxelles, B-1050 Bruxelles, Belgium*

Received 30 August 2006; accepted 20 February 2007

Abstract

In this paper, we study the competition between tumour progression due to cancer cell replication and tumour regression due to immune cell cytotoxicity. We show that the increase of specificity alone during the development of the immune response is not sufficient in general to reject the tumour. Moreover, we describe three distinct and independent mechanisms that can, in the absence of external treatment, produce regular temporally alternating phases of progression and regression: (i) a deviation from homeostasis where the population of cytotoxic cells varies; (ii) a competition for space between replicating and dead cancer cells; (iii) a formation of multi-conjugate cellular complexes where one cytotoxic cell may bind and kill several cancer cells. In the latter case, the coexistence of a low cancer cell population (interpreted as tumour dormancy) and a high population state is observed.

© 2007 Elsevier Ltd. All rights reserved.

Keywords: Solid tumour growth; Immune response; Dormancy

1. Introduction

Normal cells may lose their physiological function either spontaneously, as a result of random mutations due to ageing, or alternatively, as a result of mutations induced by chemical, physical agents or viral carcinogens. They become insensitive to factors which, under normal circumstances, limit their proliferation. Subsequently, these neoplastic cells can form progressive tumours. They are termed benign when they grow locally and respect tissue boundaries, and malignant when they invade other tissues and produce secondary tumours (or metastases) able to grow at distant sites.

Normal cells express on their surface a set of proteins, called “self-antigens”, that identify them as belonging to their original host. Except in the case of autoimmune diseases, the cells of the immune system ignore cells expressing only self-antigens (self-tolerance). However, the genetic alteration characterising tumours often generates new surface proteins in cancer cells that are not expressed by normal cells. These so-called tumour antigens can be particularly

* Corresponding author. Tel.: +44 1382 348 5369.

E-mail addresses: lejeune@maths.dundee.ac.uk (O. Lejeune), chaplain@maths.dundee.ac.uk (M.A.J. Chaplain), elakili@ulb.ac.be (I. El Akili).

effective in their ability to stimulate an immune response, or they can be weak and fail to do so. In general, a tumour contains a mixed population of cells expressing weak and strong antigens.

There is a general agreement that many spontaneous or experimental tumours, in rodents and humans, express antigens that are specific targets for immune cells, notably for cytotoxic T lymphocytes (CTL) [1–4] and for natural killers (NK) cells [5–7]. Hence, it has been argued that these immune cytotoxic cells, generally called effector cells, play a role in tumour regression and dormancy (absence of growth) in both animals and humans [8–12]. Besides cellular immunity, the involvement of humoral antibody response in the control of tumour growth has been reported [13,14]. Failure to induce angiogenesis (growth of new blood vessels) seems also to play a crucial role in dormancy [15–18].

It is important to elucidate the nonlinear mechanisms which operate at the cellular population level. If adequately manipulated, they could be used to control the switching of tumours from progressive to regressive behaviour. The intricacies of effector–target interactions make it impossible, or at best unreliable, to attempt to guess these mechanisms intuitively by extrapolating from what is known concerning the properties of individual cells. Unavoidably, there is a gap in our understanding of what is known from the processes taking place inside cells, or during cellular interactions, and what happens at the higher level of description where the evolution of cellular populations takes place. At this supracellular level, this evolution is determined by nonlinear laws whose outcome may depend on various feedback effects.

Mathematical modelling is a tool for closing this gap and for making the analysis of biological dynamical processes a less hazardous, more reliable endeavour. In regard to the highly complex processes at hand when one deals with the immune system, a mathematical model is a construct which necessarily finds its location midway between phenomenological observations and biological reality. Though it cannot accurately represent or simulate this reality, it may nevertheless, in some qualitative sense, represent a good and useful approximation. Various aspects of the immune response to cancer have been the objects of mathematical modelling for many years. The cellular compartment of the immune system in particular is a field of intensive investigation.

Models of cell-mediated immune responses against tumours can be divided into two classes: (i) those which describe the regulation processes affecting the production of effector cells and their kinetic properties [19–36]; and (ii) those in which the number of cytotoxic cells is treated as a parameter [37–41]. The interest of these studies is to determine to what extent immunoregulation processes are responsible for dynamical behaviours such as the spontaneous switch of tumour growth from progressive to regressive (and conversely) or tumour dormancy. In the last decade, investigation has focused on the mathematical modelling of spatial aspects associated with the cell-mediated immune response to cancer [42–45].

This paper discusses the kinetic properties of proliferating cancer cells attacked by CTLs. The basic cytolytic cycle shows a paradoxical behaviour, in which increasing specificity of effectors in the course of the immune response may stabilise the tumoral state (Section 2). Three distinct and independent mechanisms based on cytotoxic reactions are proposed to explain how progressive and regressive phases of the tumour may alternate spontaneously with a well defined period of time: first, the supply of effectors with a finite life time but escaping apoptosis when bound to a target (Section 3); second, the close packing effect of dead, but not yet physically eliminated cancer cells (Section 4); third, the dependence of binding and lysis rates on the conjugation state of multicellular complexes (Section 5). In the latter case, a hysteresis phenomenon appears where two tumoral states, one of low and one of high density, coexist for the same physiological condition. The realised state will depend upon the history of the system. The low density equilibrium is interpreted as a dormant state of the tumour.

2. The basic kinetic model

We consider the idealised situation of a small, growing, avascular tumour which elicits a response from the host immune system. The replicating cancer cells are attacked by activated CTLs. Kinetically speaking, all cells of a given type are identical. We also assume that their physiological environments (temperature, oxygen and nutrient concentrations, etc.) are identical. It is then meaningful to describe the average rate of cancer cell birth in term of one kinetic parameter, the replication constant r , which is independent of time. Formally, r corresponds to a “reaction step” of the form:



On the other hand, cancer cells express antigens which are specifically recognised as non-self by CTLs. These antigens consist of a peptide bound to the major histocompatibility complex (MHC) present on the surface of cancer cells. The recognition initiates a cascade of adhesion and transmembrane signaling events involving different receptors and cellular structures. The CTLs, having bound a target cell, kill it by delivering a so called “lethal hit”. This involves the production of a toxic agent or of a messenger triggering a cascade of events ending by the target cells death. In its simplest form, the corresponding cytolytic cycle may be sketched as follows [46–50]:



where E_0 , C , E_1 and H represent free effector cells, target cells, monoconjugate effector–target complexes and dead (or programmed to death) target cells, respectively.

The first binding step stands for the sequence of molecular events responsible for the recognition of the target tumoral antigens by the effector cells and for the formation, at the membrane level, of a cellular effector–target-complex. The overall rate of this process is characterised by the phenomenological kinetic constant b . The value of b is a measure of the average effector cell specificity; large values of b correspond to a high anti-tumour specificity of the receptors present on the surface of the effector cells.

The second step of (2), characterised by the phenomenological constant k , represents the lytic process in which the effector cell delivers a lethal hit triggering a sequence of events ending with the target’s death. Subsequently, the effector–target complex dissociates so that the free effector cell becomes available for a new cytolytic cycle.

The decomposition of the cytolytic cycle into at least two steps takes into account the fact that two functionally distinct structures of the effector cell participate in the cytolytic cycle: (i) the membrane receptors recognising the tumoral antigens; (ii) the cytoplasmic machinery responsible for the delivery of the lethal hit. This decomposition is further supported by the fact that different chemical agents influence independently the processes of binding and lethal hit delivery [51].

The kinetic equations describing the temporal evolution of the cellular densities read:

$$\frac{dc}{dt} = rc \left(1 - \frac{c}{K}\right) - be_0c, \tag{3}$$

$$\frac{de_0}{dt} = -be_0c + ke_1, \tag{4}$$

$$e_T = e_0 + e_1, \tag{5}$$

where c and e_i ($i = 0, 1$) represent the target and the effector densities, respectively. In the absence of cytotoxic reactions, the target population evolves according to a logistic equation, see (3). At low cellular densities, it grows exponentially; at high densities, when the cell population becomes “closely packed”, the rate of growth vanishes. The maximum achievable density K is determined by the maximum number of target cells a volume element V may contain. The space occupied by free effector cells can be neglected, because their volume ($\approx 5 \times 10^{-10} \text{ cm}^3$) is one order of magnitude smaller than the one of target cells ($\approx 5 \times 10^{-9} \text{ cm}^3$). On the other hand, the contribution of monoconjugate complexes to the close packing can also be neglected, because the cytolytic cycle (binding and lysis) is fast ($\approx 10\text{--}100 \text{ day}^{-1}$) compared to replication ($\approx 0.1\text{--}1 \text{ day}^{-1}$). The total number of effectors in V is assumed to be constant. The evolution equation of the bound effector density e_1 is derived from Eq. (4), which governs the evolution of the free effector density e_0 and from the conservation equation (5) that expresses the fact that the sum of the two effector densities is equal to a constant: e_T .

We take the interval r^{-1} between successive replications as our time unit; we take the close packing density K and the total density e_T as density units for target and effector cells, respectively. Then, on making the following substitutions:

$$\tau = rt, \quad x = \frac{c}{K}, \quad y_i = \frac{e_i}{e_T} \quad (i = 0, 1), \tag{6}$$

the equation system (3)–(5) may be re-written as

$$\frac{dx}{d\tau} = x(1 - x) - \beta y_0 x, \tag{7}$$

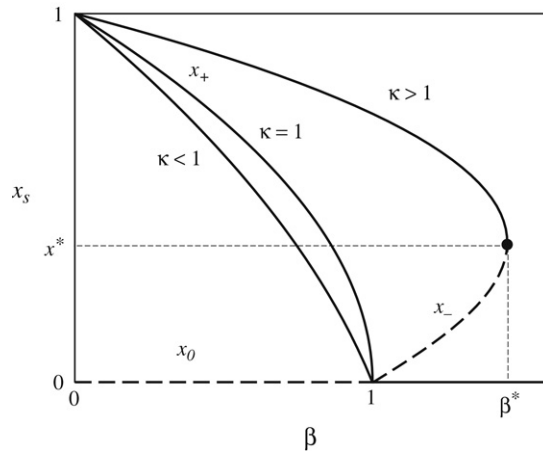


Fig. 1. Steady states x_s as a function of the switching parameter β for increasing values of κ . Stable solutions are represented by full lines and unstable ones by dashed lines. A hysteresis loop appears for $\kappa > 1$ in the range $1 \leq \beta \leq \beta^*$: the two simultaneously stable states x_0 and x_+ are separated by an intermediate unstable state x_- . The turning point (β^*, x^*) is indicated by a small black disc (●).

$$\frac{dy_0}{d\tau} = \eta(-\kappa y_0 x + y_1), \tag{8}$$

$$y_1 = 1 - y_0, \tag{9}$$

where the dimensionless combinations of parameters are

$$\beta = \frac{be_T}{r}, \quad \eta = \frac{k}{r}, \quad \kappa = \frac{bK}{k}. \tag{10}$$

The equation system (7)–(9) admits three distinct branches of steady state solutions $S \equiv (x_s, y_{0s}, y_{1s})$. The trivial one $S_0 \equiv (0, 1, 0)$ always exists and corresponds to cancer free states, where all effectors are unbound. The two other ones $S_{\pm} \equiv (x_{\pm}, y_{0\pm}, y_{1\pm})$ are given by the expressions:

$$x_{\pm} = \frac{\kappa - 1 \pm \sqrt{(\kappa - 1)^2 + 4\kappa(1 - \beta)}}{2\kappa}, \quad y_{0\pm} = \frac{1}{1 + \kappa x_{\pm}}, \quad y_{1\pm} = \frac{\kappa x_{\pm}}{1 + \kappa x_{\pm}}, \tag{11}$$

and correspond to tumoral states. The linear stability of the trivial state S_0 is determined by the eigenvalues $\omega_1 = 1 - \beta$ and $\omega_2 = -\eta$. The eigenvalues for the states S_{\pm} are the roots of the characteristic equation:

$$\omega^2 + [(1 + \eta\kappa)x_{\pm} + \eta]\omega + \eta x_{\pm}[2\kappa x_{\pm} - (\kappa - 1)] = 0. \tag{12}$$

Analysing the coefficients of this polynomial, it is straightforward to see that the sum of the eigenvalues is always negative and that their product is positive for x_+ and negative for x_- . Besides, the discriminant is never negative:

$$D = [(1 + \kappa x_{\pm})\eta - x_{\pm}]^2 + 4\eta\kappa x_{\pm}(1 - x_{\pm}) > 0, \tag{13}$$

given that the kinetic parameters are positive defined and that $0 \leq x_{\pm} \leq 1$. As a result, the eigenvalues are always real and there is no Hopf bifurcation. The eigenvalues are both negative for x_+ and of opposite sign for x_- .

The bifurcation diagram of the steady state solutions $x_s \equiv \{x_0, x_{\pm}\}$ is illustrated in Fig. 1. For $\beta < 1$, the cancer free state $x_0 = 0$ is unstable (dashed line), and any cancer cell present will develop into a growing tumour. At the switching point, $\beta = 1$, x_0 changes stability and the cancer free state becomes stable for $\beta > 1$ (full line). For $\kappa \leq 1$, the only physically acceptable (positive real) tumoral state is x_+ in the interval $0 \leq \beta \leq 1$ and it is stable. For $\kappa > 1$, this branch of stable solutions extends up to the turning point:

$$\beta^* = \frac{(\kappa + 1)^2}{4\kappa}, \quad x^* = \frac{\kappa - 1}{2\kappa}. \tag{14}$$

In the interval $1 \leq \beta \leq \beta^*$, it coexists with the branch of unstable tumoral states x_- .

That binding dominates replication, i.e. $\beta > 1$, is a necessary condition for tumour rejection by cytotoxic reactions. It is not sufficient, however, when lysis is the rate limiting step of the cytolytic cycle, $\kappa > 1$; rejection then becomes only certain beyond the turning point: $\beta > \beta^* > 1$. In the course of the immune response, both β and κ are expected to increase. The switching parameter β increases because the production of specific effectors amounts to larger binding constants b [52] and total effector densities e_T [53], while the cytolytic parameter κ increases because it is also proportional to b . Since replication and lysis are independent of binding, let us assume that r and k remain constant in the expressions of β and κ . For a given increase in specificity, i.e. for a given variation of b , the variations of β and κ may differ considerably, being in the first case proportional to e_T/r , and in the second case to $1/k$. Thus, as b increases because of the immune response, β runs against increasing values of κ .

If κ exceeds 1 before β , the tumoral states become stabilised, since now the tumoral branch x_+ extends up to $\beta^* > 1$. Whether β can overtake β^* , once $\kappa > 1$, depends upon the ratio:

$$\frac{\beta}{\beta^*} = 4\mu \frac{\kappa^2}{(1 + \kappa)^2} \quad \text{where } \mu = \frac{ke_T}{r}. \tag{15}$$

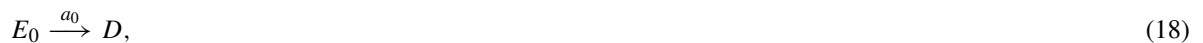
Indeed, as κ increases, this ratio tends asymptotically to 4μ . Only if this value is larger than 1, i.e. if $\mu > 1/4$, will the condition for immune rejection be met. If $\mu < 1/4$, β^* is always larger than β : the tumour outruns the immune response and remains progressive. On the other hand, the ratio $\beta/\kappa = \mu$ is a constant, so that $\mu > 1$ is the condition for which rejection will necessarily happen when the inequality $\beta > 1$ is satisfied. No hysteresis loop is involved, because β increases more rapidly than κ . When $1/4 < \mu < 1$, κ reaches 1 before β and the hysteresis loop appears. The turning point β^* , however, increases less rapidly than κ , so that for

$$\kappa > \kappa^* = \frac{1 + 2\sqrt{\mu}}{4\mu - 1}, \tag{16}$$

β overtakes β^* .

3. Deviation from homeostasis

Following [33,34], we allow now the total number of effector cells in V to vary with time. The effector density in the tissue may deviate from its homeostatic value. We assume that the tissue is supplied with mature effectors at a constant rate flow s , and that these effectors undergo apoptosis at different constant rates according to whether they are free, a_0 , or bound to a target cell, a_1 :



The flow of CTLs is assumed to be “normal”, i.e. non-enhanced by the presence of tumour cells. The dependence of apoptosis upon the conjugation state (free or bound) takes into account the possibility of an immortalisation of CTLs and/or a “counterattack” of tumour cells against CTLs in the bound state.

The kinetic equations corresponding to the reaction steps (1), (2) and (17)–(19) are

$$\frac{dc}{dt} = rc \left(1 - \frac{c}{K}\right) - be_0c + a_1e_1, \tag{20}$$

$$\frac{de_0}{dt} = s - a_0e_0 - be_0c + ke_1, \tag{21}$$

$$\frac{de_1}{dt} = be_0c - a_1e_1 - ke_1. \tag{22}$$

Time, target density are scaled according to (6) and effector densities are normalised by their equilibrium value in the absence of cytotoxic reactions:

$$y_i = \frac{a_0}{s} e_i \quad (i = 0, 1). \tag{23}$$

Then the dimensionless equations corresponding to the system (20)–(22) are

$$\frac{dx}{d\tau} = x(1 - x) - \beta \left(y_0 x - \gamma \frac{\alpha}{\kappa} y_1 \right), \tag{24}$$

$$\frac{dy_0}{d\tau} = \eta[\alpha(1 - y_0) - \kappa y_0 x + y_1], \tag{25}$$

$$\frac{dy_1}{d\tau} = \eta[\kappa y_0 x - (1 + \gamma\alpha)y_1], \tag{26}$$

where the new parameter combinations are

$$\beta = \frac{bs}{a_0 r} \quad \gamma = \frac{a_1}{a_0}, \quad \alpha = \frac{a_0}{k}, \tag{27}$$

κ and η being defined above in (10).

Eqs. (24)–(26) admit three branches of steady state solutions qualitatively equivalent to those of the system (7)–(9) that are illustrated in Fig. 1. The switching point where the cancer free state $x_0 = 0$ changes stability is now $\beta = 1 + \gamma\alpha$. The hysteresis loop exists for $\kappa > 1/\gamma + \alpha$, and the new turning point where x_+ and x_- merge is

$$\beta^* = \frac{[\gamma(\kappa + \alpha) + 1]^2}{4\gamma\kappa}, \quad x^* = \frac{\gamma(\kappa - \alpha) - 1}{2\gamma\kappa}. \tag{28}$$

Setting $\gamma = 1$ and $\alpha = 0$, Eqs. (24)–(26) reduce to the system (7)–(9) and expressions (28) become (14). It corresponds to taking the limits $s \rightarrow 0$ and $a_i \rightarrow 0$ ($i = 0, 1$) in such a way that $a_1/a_0 \rightarrow 1$ and $s/a_0 \rightarrow e_T$.

The linear stability, on the other hand, changes qualitatively. Obviously, in the limit $\gamma \rightarrow \infty$, i.e. $a_1 \rightarrow \infty$, where effectors die instantaneously when bound to a target, the tumour is monotonously increasing in mass because its growth is not hindered. For the particular value $\gamma = 1$, corresponding to a situation where apoptosis of effectors is independent of their conjugation state, $a_1 = a_0$, the characteristic polynomial equation for the tumoral states $x_s \equiv \{x_+, x_-\}$ takes the form $\omega^3 + P\omega^2 + Q\omega + R = 0$ where the coefficients can be written as

$$P = \alpha\eta + \alpha(1 - x_s + \eta) + \eta(1 + \kappa x_s) + x_s, \tag{29}$$

$$Q = \eta(\alpha^2(1 - x_s + \eta) + \alpha(2x_s + \eta(1 + \kappa x_s))) + x_s(1 - \kappa + 2\kappa x_s), \tag{30}$$

$$R = \alpha\eta^2 x_s (\alpha + 1 - \kappa + 2\kappa x_s). \tag{31}$$

The necessary and sufficient conditions to have a Hopf bifurcation are $P > 0$, $Q > 0$ and $PQ - R = 0$ (Routh–Hurwitz theorem). The inequality $P > 0$ is always satisfied since kinetic parameters are positive defined and $0 \leq x_s \leq 1$. However the two last conditions are incompatible, since

$$PQ - R = (P - \alpha\eta)(Q + \alpha^2\eta^2) = 0 \Rightarrow Q < 0, \tag{32}$$

given that $P > \alpha\eta$, see (29). As a result, there is no Hopf bifurcation.

The interesting dynamical behaviour arises in the limit $\gamma \rightarrow 0$, i.e. $a_1 \rightarrow 0$, where effectors bound to a target do not undergo apoptosis. There are only two branches of steady state solutions $S \equiv (x_s, y_{0s}, y_{1s})$. The trivial branch $S_0 \equiv (0, 1, 0)$ always exists, and becomes stable beyond the switching point $\beta = 1$ (eigenvalues are $\omega_1 = 1 - \beta$, $\omega_2 = -\eta$, and $\omega_3 = -\eta\kappa$). The other branch $S_1 \equiv (1 - \beta, 1, \kappa(1 - \beta))$ is only physically meaningful in the range $0 \leq \beta \leq 1$, where it may undergo Hopf bifurcations.

It is worthwhile to note that the dynamics of the system (24)–(26) for $\gamma = 0$ are confined to a finite box of the phase space (x, y_0, y_1) . The system, once in the region $x, y_0, y_1 \geq 0$, remains there, since all negative terms tend to zero along with the variables. It is also obvious that the variable x cannot increase beyond 1, since the only positive term of Eq. (24) vanishes for that value. Now we take a linear combination of Eqs. (24) and (26) in such a way that the terms proportional to $y_0 x$ cancel out. We find an upper bound to this combination by dropping the negative nonlinear term $-x^2/\beta$. We then add and subtract the same expression $\eta x/\beta$ and find a new upper bound using the inequality

Table 1
Kinetic constant rates are expressed per day

r (day ⁻¹)	bK (day ⁻¹)	k (day ⁻¹)	s/K (day ⁻¹)	a_0 (day ⁻¹)
10^{-1} – 1	10^2	10	10^{-5}	10^{-2}
	κ	η	β	α
	10	10 – 10^2	10^{-1} – 1	10^{-3}

The value of the carrying capacity used is $K \approx 10^9$ cells cm⁻³. Dimensionless parameters are estimated according to expressions (10) and (27).

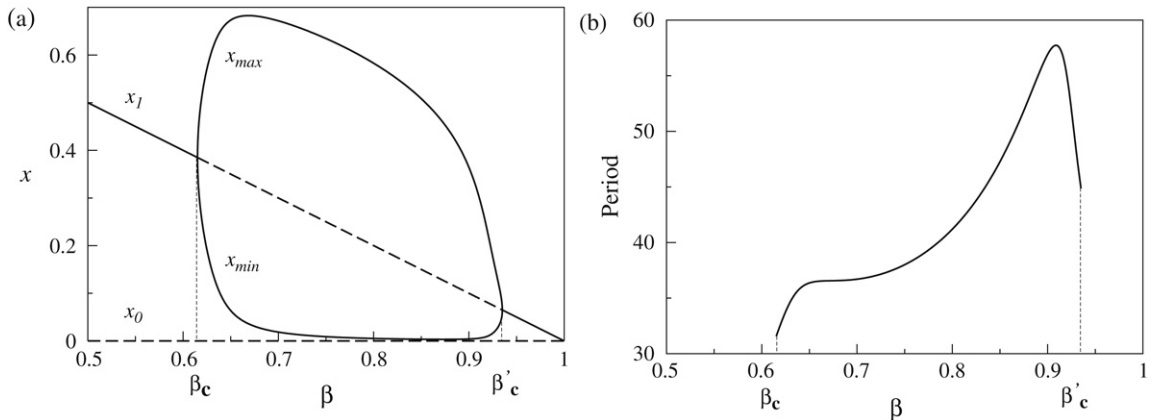


Fig. 2. Results of numerical bifurcation analysis for the parameter values $\alpha = 0.005$, $\eta = 100$ and $\kappa = 10$. (a) Tumoral states x as a function of β . Stable solutions are represented by full lines and unstable ones by dashed lines. Between the two supercritical bifurcation points β_c and β'_c , the steady state x_1 becomes unstable and gives rise to sustained oscillations characterised by a maximum value x_{max} and a minimum value x_{min} . (b) Corresponding periods of oscillation.

$x \leq 1$:

$$\frac{d}{dt} \left(\frac{x}{\beta} + \frac{y_1}{\eta\kappa} \right) \leq \frac{x}{\beta} - \frac{y_1}{\kappa} \leq \eta \left[\frac{1 + \eta}{\eta\beta} - \left(\frac{x}{\beta} + \frac{y_1}{\eta\kappa} \right) \right]. \tag{33}$$

The evolution of the linear combination of variables $x/\beta + y_1/(\eta\kappa)$ is bound from above by the expression $(1 + \eta)/(\beta\eta)$. Each positive term of the combination is less than the upper bound. As a result, we have

$$y_1 \leq (1 + \eta) \frac{\kappa}{\beta}. \tag{34}$$

We find an upper bound to the evolution of y_0 by dropping the negative term proportional to y_0x in Eq. (25) and by using the inequality (34):

$$\frac{dy_0}{dt} \leq \alpha\eta \left[1 + (1 + \eta) \frac{\kappa}{\alpha\beta} - y_0 \right] \Rightarrow y_0 \leq 1 + (1 + \eta) \frac{\kappa}{\alpha\beta}. \tag{35}$$

In order to carry out a numerical analysis of the model equations (24)–(26) for $\gamma = 0$ (i.e. $a_1 = 0$), the values of the parameters are estimated on the basis of data given in [34]. The orders of magnitude of the kinetic constants and of their dimensionless combinations are shown in Table 1. There are clearly three distinct groups of time scales: binding and lysis rates by effectors are much larger than replication rate of targets which in turn is much larger than supply and apoptosis rates of effectors.

A typical bifurcation diagram of the tumoral solutions x is shown in Fig. 2(a). The parameter values are in agreement with the orders of magnitude in Table 1. The cancer free state $x_0 = 0$ is unstable for $\beta < 1$. The branch of tumoral states $x_1 = 1 - \beta$ undergo two Hopf bifurcations at the critical points β_c and β'_c . Any slight deviation from the steady state x_1 is amplified into periodic oscillations of amplitude $A = x_{max} - x_{min}$ in the interval $\beta_c < \beta < \beta'_c$. The variation of the period as a function of the switching parameter β is shown in Fig. 2(b). Very roughly, the period

is an increasing function of the control parameter. Going back to physical dimension, this period is of the order of few months.

4. Close packing effect

Killed cancer cells give rise to a necrotic core. The constituents of the latter are assumed to dissociate and to diffuse through the tumour. The necrotic products which include cellular ingredients (such as DNA, proteins, lipids, water,...) may be used by living cancer cells to proliferate. Otherwise they can be eliminated by “housekeeping cells” such as macrophages. On the other hand, experiments have shown that the necrotic region is source of chemical substances that inhibit mitosis and that could be responsible for the growth saturation of multicellular tumour spheroids [54]. Hence, the necrotic core of the tumour could affect its growth rate. So far, however, the mechanism of dead cell elimination as well as the stimulatory and inhibitory interactions involved in this process remain poorly understood. This process is clearly independent from cytocydal reactions. It possesses its own time scale, distinct from those characterising replication, binding and lysis. We describe it by the first order reaction step:

$$H \xrightarrow{e}, \tag{36}$$

so that e^{-1} represents the average time a dead cancer cell H remains in the tumour.

The kinetic equations corresponding to the reaction steps (1), (2) and (36) are

$$\frac{dc}{dt} = rc \left(1 - \frac{c+h}{K} \right) - be_0c, \tag{37}$$

$$\frac{de_0}{dt} = -be_0c + k(e_0 - e_T), \tag{38}$$

$$\frac{dh}{dt} = k(e_0 - e_T) - eh, \tag{39}$$

where the saturation factor of the logistic term in (37) is modified to take into account the close packing effect of dead targets of density h . The total number of effectors per unit volume is again constant, so that the bound effector density is simply $e_1 = e_T - e_0$. Time, living target density, and effector densities are scaled according to (6), and dead target density is normalised by the close packing density K :

$$z = \frac{h}{K}. \tag{40}$$

Accordingly, the equation system (37)–(39) may be re-written as

$$\frac{dx}{d\tau} = x(1 - x - z) - \beta y_0 x, \tag{41}$$

$$\frac{dy_0}{d\tau} = \eta(-\kappa y_0 x + 1 - y_0), \tag{42}$$

$$\frac{dz}{d\tau} = \frac{\beta}{\kappa}(1 - y_0) - \epsilon z, \tag{43}$$

with the new dimensionless expression

$$\epsilon = \frac{e}{r}. \tag{44}$$

In the limit where dead targets are instantly eliminated, $\epsilon \rightarrow \infty$ and hence $z \rightarrow 0$ (i.e. $e \rightarrow \infty \Rightarrow h \rightarrow 0$), the system (41)–(43) becomes strictly equivalent to (7)–(9). Recalling that the cytolytic cycle of effectors is fast compared to replication of targets, we assume that y_0 equilibrates rapidly with respect to x and y , and replace adiabatically Eq. (42), i.e. $y_0 = 1/(1 + \kappa x)$, in Eqs. (41) and (43):

$$\frac{dx}{d\tau} = x(1 - x - z) - \frac{\beta x}{1 + \kappa x}, \tag{45}$$

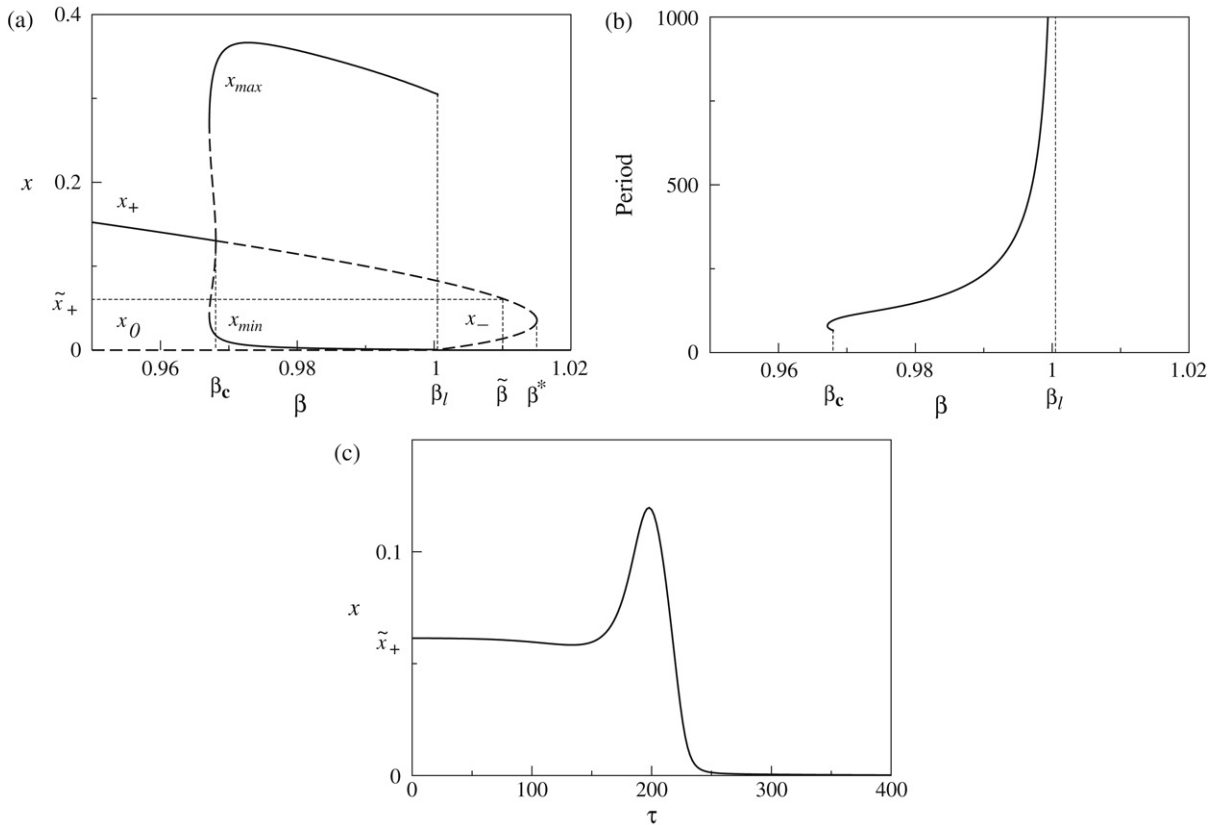


Fig. 3. Results of bifurcation analysis for the parameter values $\kappa = 12$ and $\epsilon = 0.1$. Unstable solutions are represented by dashed lines. (a) Tumoral states x as a function of β . Above the subcritical bifurcation point, $\beta > \beta_c$, the steady state x_+ becomes unstable and gives rise to sustained oscillations of amplitude $A = x_{max} - x_{min}$. The limit cycle disappears at $\beta_l > 1$. (b) Corresponding periods of oscillation. (c) Numerical integration for $\tilde{\beta} = 1.01$.

$$\frac{dz}{d\tau} = \frac{\beta x}{1 + \kappa x} - \epsilon z. \tag{46}$$

These equations admit three branches of steady state solutions qualitatively equivalent to those of the system (7)–(9) that are illustrated in Fig. 1, except that in this case the branch x_+ can change concavity. Indeed, the branch x_+ is a concave function of β for $\kappa > 1/\epsilon$, it is a straight line ($x_+ = 1 - \beta$) for $\kappa = 1/\epsilon$, and it is convex for $\kappa < 1/\epsilon$. The switching point where the cancer free state $x_0 = 0$ changes stability is still $\beta = 1$. The hysteresis loop exists for $\kappa > 1 + 1/\epsilon$, and the new turning point where x_+ and x_- merge is

$$\beta^* = \epsilon(\kappa - 1 - 2\kappa x^*), \quad x^* = -\epsilon + \sqrt{(1 + \epsilon) \left(\epsilon - \frac{1}{\kappa} \right)}, \tag{47}$$

which tends to (14) in the limit $\epsilon \rightarrow \infty$.

The bifurcation diagram of the tumoral solutions x in the hysteresis regime $\kappa > 1 + 1/\epsilon$ is shown in Fig. 3(a) (the case $\kappa \leq 1 + 1/\epsilon$ differs qualitatively from Fig. 2 only in that the steady state curves can be convex or concave). The cancer free state x_0 is unstable for $\beta < 1$, and stable otherwise. The branch of tumoral states x_+ changes stability at the Hopf critical point β_c . For $\beta_c < \beta < \beta_l$, any slight deviation from the steady state x_+ is amplified into sustained periodic oscillations characterised by a maximum value x_{max} and a minimum value x_{min} . The bifurcation is subcritical: in a small region below criticality, $\beta < \beta_c$, stable oscillations coexist with the stable state x_+ and with unstable oscillations of smaller amplitude. At the limit point $\beta_l > 1$, the branch of minima x_{min} crosses the one of unstable tumoral states x_- and the oscillations are not sustained anymore.

The variation of the period as a function of the switching parameter β is shown in Fig. 3(b). The period of stable oscillations is an increasing function of the control parameters, which diverge to infinity at the limit point β_l . The period is of the order of several months near the bifurcation point β_c . For $\beta_l < \beta < \beta^*$, the tumoral states x_+ and x_- are both unstable and there is no limit cycle; the only stable solution possible is the cancer free state x_0 . The situation is illustrated in Fig. 3(c), where a slight deviation of the tumoral population from the unstable state \tilde{x}_+ leads to extinction after an oscillation or two.

In absence of Hopf bifurcation, rejection of the tumour would occur at the turning point β^* . Thanks to the Hopf instability, rejection occurs earlier, at the limit point $\beta_l (< \beta^*)$. Let us emphasize that this is only a local rejection condition since the tumour has the potential to invade surrounding tissue.

5. Multiconjugate cellular complexes

In reality, cytotoxic reaction schemes involve many more steps than the basic cytolytic cycle (2) when effector and target cells can form multicellular complexes. Two distinct reaction pathways are then possible, depending on the effector–target number ratio. When this ratio is larger than one, the multicellular complexes are mainly constituted of a single target cell bound by several effector cells. When this ratio is smaller than one, which is generally the case *in vivo*, the multicellular complexes which form are mainly constituted of a single effector cell bound to several target cells. Following [40], the cytolytic reaction scheme is in that latter case approximated by:



where E_2 represents an effector cell bound to two target cells (2 is the maximum number of targets that an individual effector cell can bind simultaneously). The constants b_i ($i = 0, 1$) and k_i ($i = 1, 2$) are the binding and lytic kinetic constants characterising each type of effector–target complex. This simplified reaction scheme suffices in order to reveal the qualitative behaviours which may arise under those conditions. The important point is that binding and lysis rates may depend on the conjugation state, i.e. $b_0 \neq b_1$ and $k_1 \neq k_2$. As a matter of fact, *in vitro* experiments [40] point out that $b_1 \gg b_0$ and $k_2 \ll k_1$. The effector binds a second target more rapidly than the first one, but is slower to kill one of the two targets in the biconjugate state (E_2) than the single target in the monoconjugate state (E_1). When an effector cell is already bound to a target cell, the activation time of its membrane receptors for the recognition and binding of the surface antigens of a new target cell is spared. On the contrary, the mobilisation of cytoplasmic structures of the effector cell to deliver a lethal hit to two different target cells in parallel takes more time.

The kinetic equations corresponding to the reaction steps (1) and (48) are

$$\frac{dc}{dt} = rc \left(1 - \frac{c}{K} \right) - 2b_0e_0c - b_1e_1c, \tag{49}$$

$$\frac{de_0}{dt} = -2b_0e_0c + k_1e_1, \tag{50}$$

$$\frac{de_1}{dt} = 2b_0e_0c - b_1e_1c - k_1e_1 + 2k_2e_2, \tag{51}$$

$$e_T = e_0 + e_1 + e_2. \tag{52}$$

The combinatorial factor 2 expresses the assumption that effector cells behave as if they have only two receptors. Time, target density are scaled according to (6) and effector densities are normalised by their total density e_T :

$$y_i = \frac{e_i}{e_T} \quad (i = 0, 1, 2). \tag{53}$$

Then the dimensionless equations corresponding to the system (49)–(52) are

$$\frac{dx}{d\tau} = x(1 - x) - \beta \left(y_0 + \frac{1}{2}\rho y_1 \right) x, \tag{54}$$

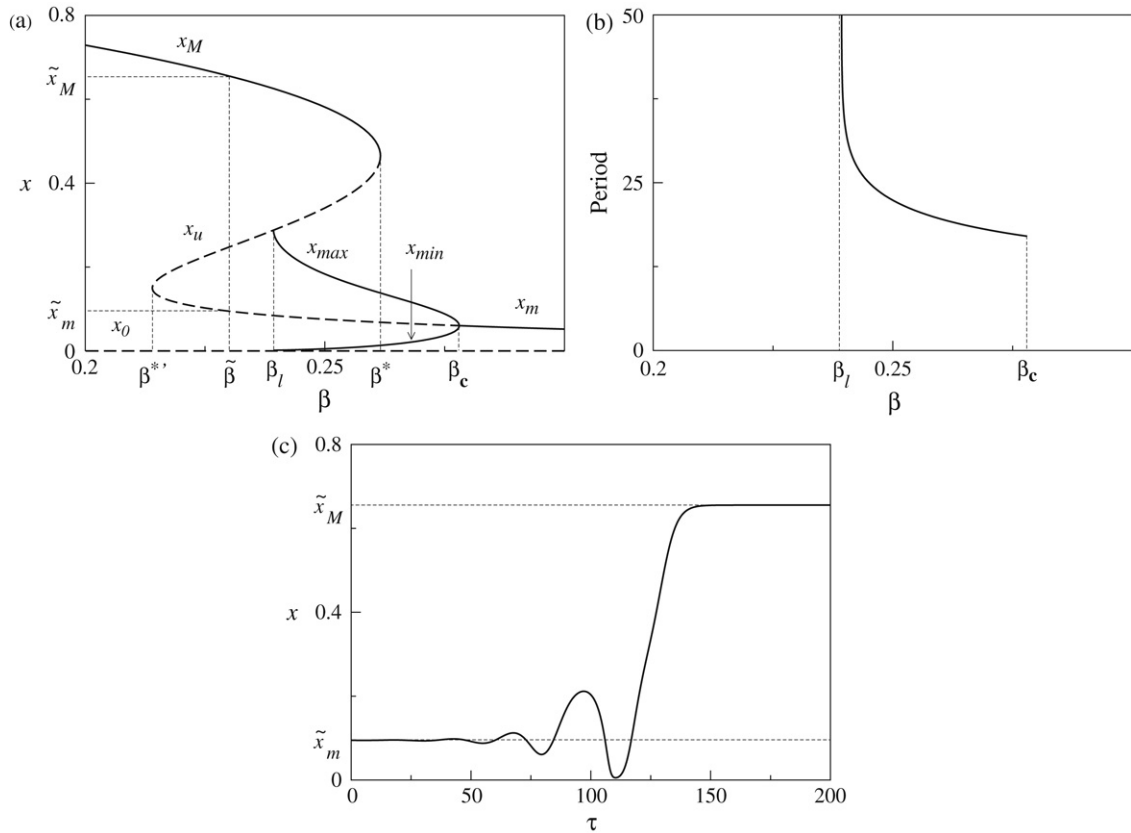


Fig. 4. Results of bifurcation analysis for the parameter values $\rho = 10^3$, $\eta = 10$, $\kappa_1 = 0.05$ and $\kappa_2 = 10^3$. Unstable solutions are represented by dashed lines. (a) Tumoral states x as a function of β . Below the supercritical bifurcation point, $\beta < \beta_c$, the steady state x_m becomes unstable and gives rise to sustained oscillations of amplitude $A = x_{max} - x_{min}$. The limit cycle disappears at β_l . (b) Corresponding periods of oscillation. (c) Numerical integration for $\tilde{\beta} = 0.23$.

$$\frac{dy_0}{d\tau} = \eta(-2\kappa_1 y_0 x + y_1), \tag{55}$$

$$\frac{dy_1}{d\tau} = \eta \left[2\kappa_1 y_0 x - (1 + \rho\kappa_1 x)y_1 + 2\rho \frac{\kappa_1}{\kappa_2} y_2 \right], \tag{56}$$

$$y_2 = 1 - y_0 - y_1 \tag{57}$$

where the dimensionless combinations of parameters are

$$\beta = 2 \frac{b_0 e_T}{r}, \quad \rho = \frac{b_1}{b_0}, \quad \eta = \frac{k_1}{r}, \quad \kappa_i = \frac{b_{i-1} K}{k_i} \quad (i = 1, 2). \tag{58}$$

In the limits, $\rho \rightarrow 0$, $\kappa_2 \rightarrow \infty$ and $y_2 \rightarrow 0$ such that $\rho/\kappa_2 \rightarrow \text{constant} \neq 0$ (i.e. $b_1 \rightarrow 0$, $\kappa_2 \rightarrow \infty$ and $e_2 \rightarrow 0$), the system (54)–(57) reduces to (7)–(9).

There are four branches of steady state solutions. A new situation may arise where three distinct tumoral states coexist with the cancer free state for the same parameter values. The case is illustrated in Fig. 4(a). Parameter values are chosen in agreement with data given in [40], according to which $\rho, \eta, \kappa_2 \gg 1$ and $\kappa_1 \ll 1$. For $\beta < \beta^*$, the high density x_M , referred to as macro-tumoral state, is the only steady solution different from zero. For $\beta > \beta^*$, the only nontrivial steady solution is the low density one x_m referred to as micro-tumoural state. For $\beta^* < \beta < \beta_c$, the macro-tumoural and micro-tumoural states coexist with the intermediate tumoural state x_u .

The trivial state $x_0 = 0$ is unstable. The upper branch of steady states x_M is stable, and the intermediate one x_u is unstable. The lower branch x_m changes stability at the Hopf bifurcation point β_c . For $\beta_l < \beta < \beta_c$, any slight

deviation from the steady state x_m is amplified into sustained periodic oscillations characterised by a maximum value x_{\max} and a minimum value x_{\min} . At the limit point $\beta_l (> \beta^{*'})$, the branch of minima x_{\min} crosses the one of intermediate unstable states x_u , and the oscillations are not sustained anymore. In the interval $\beta_l < \beta < \beta^*$, stable oscillations around the micro-tumoural state x_m coexist with the stable macro-tumoural state x_M .

The variation of the period of oscillations as a function of the switching parameter β is shown in Fig. 4(b). The period this time is a decreasing function of the control parameter, which admits a vertical asymptote at the limit point β_l . The period is of the order of few months near the bifurcation point β_c . For $\beta^{*'} < \beta < \beta_l$, the states x_0 , x_m and x_u are all unstable and there is no limit cycle; the only stable solution possible is the macro-tumoural state x_M . The situation is illustrated in Fig. 4(c), where a slight deviation from the micro-tumoural state \tilde{x}_m leads to the macro-tumoural state \tilde{x}_M after few oscillations.

Multiconjugate cellular complexes characterised by different binding and lysis kinetic constants are responsible for the existence of an equilibrium state of low cancer cell density which can be interpreted as tumour dormancy. This dormant state may lose its stability through a Hopf bifurcation and give rise to sustained oscillations. The resulting limit cycle may in turn disappear, so that a jump to a fully blown state is observed.

6. Discussion and conclusions

The competition between cancer cell proliferation and immune cell-mediated cytotoxic reactions is modelled within the framework of kinetic equations borrowed from chemistry. On that basis, we show that although a tumour may stimulate the immune system and become the object of a specific attack by effector cells, its rejection is not certain. Depending on the evolution of the effector population in term of their number, and their binding and lysis rates in the course of the immune response, the tumour may regress and finally be rejected, or stabilise. Indeed, it is known that binding and lysis are independent processes involving completely different cellular structures (membrane and cytoplasm). It is likely that their kinetic parameters evolve independently during the immune response. Strikingly, this creates a paradoxical dynamic situation where the production of highly specific effector cells, which is obviously necessary for binding the cancer cells and a prerequisite for killing them, has, in the end for effect, to diminish the overall efficiency of the cytolytic cycle.

The dynamics of replicating targets attacked by effectors does not present oscillatory behaviour when the effector population is constant, the dead targets are instantaneously eliminated, and the cellular complexes are only monoconjugates formed by one effector bound to one target. The dynamics are, however, already complex enough to show a hysteresis phenomenon, where a tumoural state and a cancer free state are both stable for the same physiological parameter values. The realisation of one or the other state depends on the history of the system. When the supply of effectors in the malignant tissue and their apoptosis are considered, we have shown that Hopf bifurcations generating sustained oscillations in the effector and target populations exist, providing that effectors escape apoptosis when bound to a target (only free effectors die). The period of oscillation is of the order of few months.

When the elimination of the necrotic core is slow with respect to cancerous proliferation, so that its close packing effect on tumour growth cannot be neglected anymore, tumoural states may also become unstable through a Hopf bifurcation. The period of oscillation is an increasing function of the control parameter measuring the development of the immune response, and is of the order of several months near bifurcation points. In the hysteresis regime, the limit cycle disappears when the minimum value of oscillations reaches the unstable intermediate state of the loop. At that point, the period diverges to infinity. As a result, the (local) tumour rejection occurs earlier in the course of the immune response than it would without the Hopf instability. The bifurcation may be subcritical: stable oscillations coexist with unstable oscillations of smaller amplitude and with the stable tumoural steady state.

When multiconjugate cellular complexes characterised by different binding and lysis kinetic constants are considered, a new hysteresis phenomenon occurs. A high density or macro-tumoural equilibrium and a low density or micro-tumoural equilibrium may coexist in the same physiological state. The former corresponds to an “uncontrolled” tumour, while the later is interpreted as a dormant tumour. This interpretation is in agreement with experimental results according to which cell-mediated immune attack may play an important role in the induction and maintenance of cancer dormancy [11,12]. The main alternative mechanism is the balance between proliferation and apoptosis in absence of vascularisation [15–18]. The micro-tumoural state may be destabilised via a Hopf bifurcation. In contrast with previous situations, the period of oscillation is a decreasing function of the control parameter. As the efficiency

of the immune response decreases, the limit cycle ceases to exist and the density jumps to the macro-tumoural state before the (left) turning point of the hysteresis loop is reached.

In conclusion, let us stress that the involvement of T cell compartments of the immune system in anti-tumour responses is well demonstrated both in rodents and humans. Recent studies show that variable numbers of tumour-infiltrating lymphocytes are found in patients suffering from cancers. These cells can be isolated *in vitro* and studied for their functional properties. Their use in tumour immunotherapy is at present the object of intensive investigations. From this perspective, the knowledge of the kinetic parameters that characterise binding, lysis and apoptosis of effector cells as well as replication and elimination after lysis of cancer cells provide crucial information for predicting tumour evolution and in particular for estimating the conditions leading to rejection. The results presented provide a simple approach to the theoretical aspect of this problem. They also strikingly illustrate that without mathematical modelling, there is little chance of arriving, by purely intuitive reasoning, at a correct and complete picture of what is (or could be) going on *in vivo*, even in regard to the most elementary aspects of the competition between tumour growth and immune response considered here.

Acknowledgments

The authors MAJC and OL gratefully acknowledge the support by the European Community, through the Marie Curie Research Training Network Project HPRN-CT-2004-503661: Modelling, Mathematical Methods and Computer Simulation of Tumour Growth and Therapy. MAJC and OL also gratefully acknowledge helpful discussions with Prof. R. Lefever and Prof. B. Perthame.

References

- [1] P.D. Greenberg, Adoptive T cell therapy of tumors: Mechanisms operative in the recognition and elimination of tumor cells, *Adv. Immunol.* 49 (1991) 281–349.
- [2] T. Boon, J.C. Cerottini, B. Van den Eynde, P. Van der Bruggen, P. Van Pel, Tumor antigens recognized by T lymphocytes, *Annu. Rev. Immunol.* 12 (1994) 337–365.
- [3] T. Boon, P. Van der Bruggen, Human tumor antigens recognized by T lymphocytes, *J. Exp. Med.* 183 (1996) 725–729.
- [4] B. Van Den Eynde, P. Van Der Bruggen, T cell defined tumor antigens, *Curr. Opin. Immunol.* 9 (1997) 684–693.
- [5] R.B. Herberman, C.W. Reynolds, J.R. Ortaldo, Mechanism of cytotoxicity of natural killer cells, *Annu. Rev. Immunol.* 4 (1986) 651–680.
- [6] S. Kausalya, S.P. Hegde, J.J. Bright, A. Khar, Mechanism of antibody dependent naturel killer mediated AK-5 tumor cell death, *Exp. Cell Res.* 212 (1994) 285–290.
- [7] A. Khar, Mechanisms involved in natural killer cell mediated target cell death leading to spontaneous tumor regression, *J. Biosci.* 22 (1997) 23–31.
- [8] E.F. Wheelock, K.J. Weinhold, J. Levich, The tumor dormant state, *Adv. Cancer Res.* 34 (1981) 107–140.
- [9] T.H.M. Stewart, A.C. Hollinshead, S. Raman, Tumor dormancy initiation, maintenance and termination in animals and humans, *Canad. J. Surg.* 34 (1991) 321–325.
- [10] E. Zorn, T. Hercent, A naturel cytotoxic T cell response in a spontaneously regressing human melanoma targets a neoantigen resulting from a somatic point mutation, *Eur. J. Immunol.* 29 (1999) 592–601.
- [11] J.D. Farrar, K.H. Katz, J. Windsor, G. Thrush, R.H. Scheuermann, J.W. Uhr, N.E. Street, Cancer dormancy. VII. A regulatory role for CD8⁺ T cells and IFN- γ in establishing and maintaining the tumor-dormant state, *J. Immunol.* 162 (1999) 2842–2849.
- [12] V. Schirmacher, T-cell immunity in the induction and maintenance of a tumour dormant state, *Sem. Cancer Biol.* 11 (2001) 285–295.
- [13] A.J.T. George, A.L. Tutt, F.K. Stevenson, Anti-idiotype mechanisms involved in suppression of a mouse B cell lymphoma BCL, *J. Immunol.* 138 (1987) 628–634.
- [14] J.W. Uhr, T. Tucker, R.D. May, H. Siu, E.S. Vitetta, Cancer dormancy: Studies of the murine BCL₁ lymphoma, *Cancer Res.* 51 (Suppl.) (1991) 5045s–5053s.
- [15] J. Folkman, Angiogenesis in cancer, vascular, rheumatoid and other disease, *Nature Med.* 1 (1995) 27–32.
- [16] L. Holmgren, M.S. O'Reilly, J. Folkman, Dormancy of micrometastases: Balanced proliferation and apoptosis in the presence of angiogenesis suppression, *Nature Med.* 1 (1995) 149–153.
- [17] N. Bouck, V. Stellmach, S.C. Hsu, How tumours become angiogenic, *Adv. Cancer Res.* 69 (1996) 135–174.
- [18] R.L. Barnhill, M.W. Piepkorn, A.J. Cochran, E. Flynn, T. Karaoli, J. Folkman, Tumour vascularity, proliferation, and apoptosis in human melanoma micrometastases and macrometastases, *Arch. Dermatol.* 134 (1998) 991–994.
- [19] Z. Grossman, G. Berke, Tumor escape from immune elimination, *J. Theoret. Biol.* 83 (1980) 267–296.
- [20] R.J. De Boer, P. Hogeweg, Tumor escape from immune elimination: Simplified precursor bound cytotoxicity models, *J. Theoret. Biol.* 113 (1985) 719–736.
- [21] R.J. De Boer, P. Hogeweg, Interactions between macrophages and T-lymphocytes: Tumor sneaking through intrinsic to helper T cell dynamics, *J. Theoret. Biol.* 120 (1986) 331–354.
- [22] N. Bellomo, G. Forni, Dynamics of tumor interaction with the host immune-system, *Math. Comput. Modelling* 20 (1994) 107–122.

- [23] J.A. Adam, N. Bellomo (Eds.), *A Survey of Models on Tumour Immune Systems Dynamics*, Birkhäuser, Boston, 1996.
- [24] N. Bellomo, E. De Angelis, Strategies of applied mathematics towards an immuno-mathematical theory on tumors and immune system interactions, *Math. Models Methods Appl. Sci.* 8 (1998) 1403–1429.
- [25] N. Bellomo, B. Firmani, L. Guerri, Bifurcation analysis for a nonlinear system of integro-differential equations modelling tumor-immune cells competition, *Appl. Math. Lett.* 12 (1999) 39–44.
- [26] N. Bellomo, L. Preziosi, Modelling and mathematical problems related to tumor evolution and its interaction with the immune system, *Math. Comput. Modelling* 32 (2000) 413–452.
- [27] N. Bellomo, A. Bellouquid, E. De Angelis, The modelling of the immune competition by generalized kinetic (Boltzmann) models: Review and research perspectives, *Math. Comput. Modelling* 37 (2003) 65–86.
- [28] N. Bellomo, E. De Angelis (Eds.), Modeling and simulation of tumour development, treatment, and control, *Math. Comput. Modelling* 37 (2003), 1121–1252.
- [29] N. Bellomo, E. De Angelis, L. Preziosi, Multiscale modeling and mathematical problems related to tumour evolution and medical therapy, *J. Theoret. Med.* 5 (2003) 111–136.
- [30] N. Bellomo, A. Bellouquid, M. Delitala, Mathematical topics on the modelling complex multicellular systems and tumor immune cells competition, *Math. Models Methods Appl. Sci.* 14 (2004) 1683–1733.
- [31] E. De Angelis, P.E. Jabin, Mathematical models of therapeutical actions related to tumour and immune system competition, *Math. Models Methods Appl. Sci.* 28 (2005) 2061–2083.
- [32] V.A. Kuznetsov, A mathematical model for the interaction between cytotoxic lymphocytes and tumor cells. Analysis of the growth, stabilization and regression of the B cell Lymphoma in mice chimeric with respect to the major histocompatibility complex, *Biomed. Sci.* 2 (1991) 465–476.
- [33] V.A. Kuznetsov, I.A. Makalkin, M.A. Taylor, A.S. Perelson, Non-linear dynamics of immunogenic tumors: Parameter estimation and global bifurcation analysis, *Bull. Math. Biol.* 56 (1994) 295–321.
- [34] A. Matzavinos, M.A.J. Chaplain, V.A. Kuznetsov, Mathematical modelling of the spatio-temporal response of cytotoxic T-lymphocytes to a solid tumour, *Math. Med. Biol.* 21 (2004) 1–34.
- [35] A. Matzavinos, M.A.J. Chaplain, Travelling-wave analysis of a model of the immune response to cancer, *C. R. Biol.* 327 (2004) 995–1008.
- [36] Z. Szymańska, Analysis of immunotherapy models in the context of cancer dynamics, *Appl. Math. Comput. Sci.* 13 (2003) 407–418.
- [37] R. Garay, R. Lefever, A kinetic approach to immunology of cancer: Stationary states properties of effector–target cell reactions, *J. Theoret. Biol.* 73 (1978) 417–438.
- [38] S.J. Merrill, S. Sathanathan, Approximate Michaelis–Menten kinetics displayed in a stochastic model of cell-mediated cytotoxicity, *Math. Biosci.* 80 (1986) 223–238.
- [39] J.R. Hiernaux, R. Lefever, C. Uyttenhove, T. Boon, Tumor dormancy as a result of simple competition between tumor cells and cytotoxic effector cells, in: G.W. Hoffmann, J.G. Levy, G.T. Nepom (Eds.), *Paradoxes in Immunology*, CRC Press, Boca Raton, Florida, 1986, pp. 95–109.
- [40] R. Lefever, J. Hiernaux, J. Urbain, P. Meyers, On the kinetics and optimal specificity of cytotoxic reactions mediated by T-lymphocyte clones, *Bull. Math. Biol.* 59 (1992) 263–294.
- [41] J.A. Adam, The dynamics of growth-factor-modified immune response to cancer growth: One dimensional models, *Math. Comput. Modelling* 17 (1993) 83–106.
- [42] M.R. Owen, J.A. Sherratt, Pattern formation and spatio-temporal irregularity in a model for macrophage–tumour interactions, *J. Theoret. Biol.* 189 (1997) 63–80.
- [43] M.R. Owen, J.A. Sherratt, Modelling the macrophage invasion of tumours: Effects on growth and composition, *IMA J. Math. Appl. Med. Biol.* 15 (1998) 165–185.
- [44] M.R. Owen, J.A. Sherratt, Mathematical modelling of macrophage dynamics in tumours, *Math. Models Methods Appl. Sci.* 9 (1999) 513–539.
- [45] C.E. Kelly, R.D. Leek, H.M. Byrne, S.M. Cox, A.L. Harris, C.E. Lewis, Modelling macrophage infiltration into avascular tumours, *J. Theoret. Med.* 4 (2002) 21–38.
- [46] E. Grimm, B. Bonavida, Mechanism of cell-mediated cytotoxicity at the single cell level. I. Estimates of cytotoxic T lymphocyte frequency and relative lytic efficiency, *J. Immunol.* 123 (1979) 2861–2869.
- [47] D. Zagury, J. Bernard, P. Jeannesson, N. Thiernes, J.C. Cerottini, Studies on the mechanism of T cell-mediated lysis at the single effector cell level. I. Kinetic analysis of lethal hits and target cell lysis in multicellular conjugates, *J. Immunol.* 123 (1979) 1604–1609.
- [48] A.S. Perelson, G.I. Bell, Delivery of lethal hits by cytotoxic T lymphocytes in multicellular conjugates occurs sequentially but at random times, *J. Immunol.* 129 (1982) 2796–2801.
- [49] G. Berke, D. Rosen, Are lytic granules and perforin 1 involved in lysis induced by *in vivo* primed peritoneal exudate cytolytic T lymphocytes? *Transplant. Proc.* 19 (1987) 412–416.
- [50] J.D.E. Young, C.C. Liu, Multiple Mechanisms of lymphocyte-mediated killing, *Immunol. Today* 9 (1988) 140–144.
- [51] P. Golstein, C. Foa, I.C.M. Mac Lennan, Mechanism of T cell-mediated cytolysis: The differential impact of cytochalasins at the recognition and lethal hit stages, *Eur. J. Immunol.* 8 (1978) 302–309.
- [52] N. Moscovitch, Z. Grossman, D. Rosen, G. Berke, Maturation of cytolytic T lymphocytes, *Cellular Immunol.* 102 (1986) 52–67.
- [53] U. Zangemeister-Witke, B. Kyewski, V. Schirmacher, Recruitment and activation of tumor-specific immune T cells *in situ*, *J. Immunol.* 143 (1989) 379–385.
- [54] J.P. Freyer, Role of necrosis in regulating the growth saturation of multicellular spheroids, *Cancer Res.* 48 (1988) 2432–2439.